Kinetic growth percolation: Epidemic processes with immunization

Toshiya Ohtsuki and Thomas Keyes
Department of Chemistry, Boston University, Boston, Massachusetts 02215
(Received 5 August 1985)

Nonequilibrium phase transitions of kinetic growth percolation, a kinetic growth process which exhibits a percolating-nonpercolating phase transition, are investigated on the basis of a mean-field theory and/or a real-space renormalization-group method. Phase diagrams, critical exponents, and spreading velocities are calculated explicitly for several models describing epidemic processes with immunization or autocatalytic chemical reactions. The existence and the nature of phase transitions and critical behavior are clarified.

I. INTRODUCTION

In recent years the kinetic growth of random clusters, which describes chemical reactions, epidemic processes, forest fires, etc., has received considerable attention.[1-7] It has been shown that some processes belong to the same universality class as ordinary (isotropic) or directed percolation.[1-6] Here we use the terminology of epidemic processes but the following processes can also be described as autocatalytic chemical reactions. In the last section, we discuss this again. Each site (individual) can be susceptible, infected, or immune. We start with one infected site and construct a cluster step by step. Infected sites infect their nearest-neighbor susceptible sites with probability p. At the same time, they become immune with probability unity. When immunization is perfect and immune sites are never reinfected, the process is equivalent to the usual bond percolation and there exists a threshold p_c such that the probability of infinite spreading of the disease is zero below p_c and nonzero above p_c.[1-3] On the other hand, it is known that some chemical reactions (Schlögl's first model[8]) are equivalent to directed percolation.[4-6] In epidemic processes, this corresponds to the case without immunization where infected sites recover and return to the susceptible state with probability unity. Note that the d-dimensional process is equivalent to $(d+1)$-dimensional directed percolation where the additional one dimension corresponds to time in the process. Extension and generalization are straightforward. For instance, consider an imperfect immunization (resistance) process where immune sites can be reinfected with probability r. Obviously, the special cases $r=0$ and $r=p$ are equal to the perfect and no-immunization processes (isotropic and directed percolation), respectively. What happens at $p>r>0$ or $r>p$? This problem was first addressed by Cardy,[7] but little is known about the general properties of phase transitions. A wide variety of growth phenomena is considered to exhibit similar behavior where the main issue is whether a cluster spreads infinitely or not. We call this kind of process kinetic growth percolation (KGP).

The study of KGP is considered to be interesting and significant from a number of points of view. First, KGP is a good model of real growth processes ranging from chemical reactions to epidemic processes. Second, it is closely related to many subjects of much current interest, among which are (i) application of percolation theories to various dynamic processes, e.g., flow in porous media (invasion percolation), flame propagation (stirred percolation), and galactic evolution,[9] (ii) kinetic growth of fractal objects such as diffusion-limited aggregation,[10] (iii) nonequilibrium phase transitions and pattern formation,[11] and (iv) (stochastic) cellular automata.[12] KGP provides a typical example of these phenomena. The purpose of this paper is to investigate KGP and to clarify the nature of phase transitions. In this work we deal with two models, both of which contain perfect and no-immunization processes as special cases. One is a partial immunization process where perfect immunization occurs partially, i.e., infected sites are immunized perfectly with probability u and return to susceptible sites with probability $1-u$. Here perfect and no-immunization processes are described by $u=1$ and $u=0$. The other is the imperfect immunization process mentioned before. In Sec. II phase diagrams and critical behavior of partial and imperfect immunization processes are investigated on the basis of a mean-field approximation. The next two sections are devoted to a real-space renormalization-group (RSRG) approach. In the kinetics of cluster growth, a spreading velocity of a cluster or equivalently a time derivative of a cluster size is the most fundamental and important quantity. In Sec. III, therefore, we study the critical behavior of the spreading velocity in perfect and no-immunization processes. Phase diagrams and the tricritical behavior of partial and imperfect immunization processes are treated in Sec. IV. Finally, in Sec. V we summarize and discuss our results.

II. MEAN-FIELD THEORY

A. Partial immunization process

Within a framework of a mean-field approximation, all spatial fluctuations are neglected and the densities of each site become spatially constant. Temporal evolution of the partial immunization process is governed by

$$\dot{X}=(1-u)Y-cpXY\ , \tag{2.1}$$

$$\dot{Y}=-Y+cpXY\ , \tag{2.2}$$

$$\dot{Z}=uY\ , \tag{2.3}$$

where c is a coordination number and X, Y, and Z are the densities of susceptible, infected, and immune sites, respectively. The term $cpXY$ describes infection of susceptible sites by nearest-neighbor infected sites and the terms uY and $(1-u)Y$ represent immunization and recovery of infected sites. Although there is only one stationary solution,

$$Y=0\ , \tag{2.4}$$

the equation system (2.1)—(2.3) exhibits a phase transition. Consider an initial-value problem under the initial conditions

$$X(0)=1-\delta,\quad Y(0)=\delta,\quad Z(0)=0\quad(\delta\ll 1)\ ; \tag{2.5}$$

that is, only a small fraction of sites are infected at $t=0$. Substituting Eq. (2.3) into Eq. (2.1) and integrating it, we have

$$X-(1-u)/cp=A\exp(-cpZ/u)\ . \tag{2.6}$$

The initial condition (2.5) gives

$$A=1-\delta-(1-u)/cp\ . \tag{2.7}$$

On the other hand, the sum of Eqs. (2.1)—(2.3) leads to

$$X+Y+Z=1\ . \tag{2.8}$$

From Eqs. (2.6)—(2.8), we find

$$\dot{Z}=u(1-Z-(1-u)/cp)-u(1-\delta-(1-u)/cp)\times\exp(-cpZ/u)\ . \tag{2.9}$$

When $cpZ/u\ll 1$, we can expand $\exp(-cpZ/u)$ in a power series of cpZ/u and get

$$\dot{Z}=u\delta+(cp-1)Z-(cp/2u)(cp-1+u)Z^2\ . \tag{2.10}$$

Here we omit higher-order terms like δZ and Z^3. Equation (2.10) shows that for $cp<1$, $\dot{Z}<u\delta$ and Z stays at the order of δ. Note that higher-order terms in Z are negligible in this case. This means finite spreading of the disease, because the asymptotic density $Z(\infty)$ of immune sites is in proportion to the initial density δ of infected sites. At $cp>1$, in contrast, Z can grow up to the order of δ^0 and the disease can spread infinitely. The threshold p_c is given by

$$p_c=c^{-1}\ . \tag{2.11}$$

Figure 1(a) shows a phase diagram.

Near p_c as $\epsilon\equiv|p-p_c|/p_c\ll 1$, solutions of Eq. (2.10) become

$$Z(t)=(u\delta/\epsilon)(1-e^{-\epsilon t})\quad(p<p_c)\ , \tag{2.12}$$

$$Z(t)=2\epsilon(1-e^{-\epsilon t})/[1+(2\epsilon^2/u\delta)e^{-\epsilon t}]\quad(p>p_c)\ . \tag{2.13}$$

Below p_c, $Z(\infty)/\delta$ represents a mean cluster size, while above p_c, $Z(\infty)$ stands for a probability of belonging to the infinite cluster. Then Eqs. (2.12) and (2.13) "inform" us that critical exponents β and γ (Ref. 13) are independent of u and equal to unity:

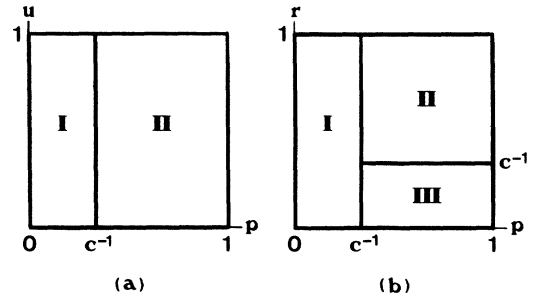

FIG. 1. Phase diagrams using the mean-field theory. (a) Partial immunization process. (b) Imperfect immunization process.

$$\beta=\gamma=1\ . \tag{2.14}$$

A relaxation time τ is also evaluated from Eqs. (2.12) and (2.13) as

$$\tau\simeq\epsilon^{-1}\quad(p<p_c)\ , \tag{2.15}$$

$$\tau\simeq\epsilon^{-1}\ln(2\epsilon^2/u\delta)\quad(p>p_c,\ \delta\to 0)\ . \tag{2.16}$$

It follows that

$$\psi=1\ , \tag{2.17}$$

where ψ is a critical exponent defined by $\tau\propto\epsilon^{-\psi}$.[1,6]

B. Imperfect immunization process

Equations of motion for the imperfect immunization process are written as

$$\dot{X}=-cpXY\ , \tag{2.18}$$

$$\dot{Y}=-Y+cpXY+crZY\ , \tag{2.19}$$

$$\dot{Z}=Y-crZY\ . \tag{2.20}$$

In this case, Eqs. (2.18)—(2.20) have two stationary solutions,

$$Y=0\ , \tag{2.21}$$

$$X=0,\quad Y=1-1/cr,\quad Z=1/cr\quad(cr>1)\ , \tag{2.22}$$

and show a little complicated behavior. As before, we solve Eqs. (2.18)—(2.20) under the initial condition (2.5). Eliminating Y from Eqs. (2.18) and (2.20) and integrating it, we get

$$Z-1/cr=AX^{r/p}\ , \tag{2.23}$$

where an integration constant A is given by

$$A=-(1-\delta)^{-r/p}/cr\ . \tag{2.24}$$

Substitution of Eqs. (2.8) and (2.24) into Eq. (2.23) yields

$$\dot{Z}=(1-crZ)[1-Z-(1-crZ)^{p/r}(1-\delta)]\ . \tag{2.25}$$

When $crZ\ll 1$, we can linearize Eq. (2.25) and obtain

$$\dot{Z}=\delta+(cp-1)Z-(c^2p^2+c^2pr-2cr)Z^2/2\ . \tag{2.26}$$

The same argument as that for the partial immunization process shows that at $cp<1$, Z remains at the order of δ

and only finite spreading of the disease occurs. For $cp>1$, the disease can spread infinitely, but two different phases appear. One is the case $cr>1$, where the stationary (asymptotic) solution is given by Eq. (2.22), and the other is the case $cr<1$ with the stationary solution Eq. (2.21). A phase diagram is plotted in Fig. 1(b). In the former phase, denoted II, both infected and immune sites can spread infinitely and survive forever. In phase III the infinite cluster of immune sites can be formed, but infected sites vanish. This suggests that during the formation of the cluster, infected sites exist only in the perimeter. This point is shown more clearly in Sec. IV.

By solving Eq. (2.26), we can calculate critical behavior in the vicinity of the phase boundary $\epsilon_p \equiv |p-p_c|/p_c \ll 1$ $(p_c=c^{-1})$,

$$Z(\infty)\propto \delta\epsilon_p^{-1} \quad (p<p_c) , \tag{2.27}$$

$$Z(\infty)\propto \epsilon_p \quad (p>p_c,\ r<r_c=c^{-1}) , \tag{2.28}$$

$$\tau\propto \epsilon_p^{-1} . \tag{2.29}$$

In phase II $(p>p_c,\ r>r_c)$, $Z(\infty)=1/cr$ is the order of unity. Thus, we cannot do linearization and cannot get an analytical solution. Note that $Z(\infty)$ shows discontinuity on the boundary $p=p_c$ $(r>r_c)$. Critical behavior near the boundary $\epsilon_r \equiv |r-r_c|/r_c \ll 1$ is also derived from equations for X and Y corresponding to Eq. (2.25),

$$\dot{X}=(p/r)[(1-cr)X+crX^2-(1-\delta)^{-r/p}X^{1+r/p}] , \tag{2.30}$$

$$(\dot{Y}/Y+crY-cr+1)/(cp-cr) = [cp(r\dot{Y}/pY+crY-cr+1)/(cp-cr)]^{p/r}(1-\delta) . \tag{2.31}$$

The results are

$$X(\infty)\propto \epsilon_r^{cp} \quad (r<r_c) , \tag{2.32}$$

$$Y(\infty)\propto \epsilon_r \quad (r>r_c) , \tag{2.33}$$

$$\tau\propto \epsilon_r^{-1} \quad (r>r_c) . \tag{2.34}$$

In phase III $(r<r_c)$ the time dependence of X cannot be obtained analytically, because linearization is not applicable. Notice that the present calculation leads to the exponent cp for $X(\infty)$, which depends on the value of p.

III. REAL-SPACE RENORMALIZATION-GROUP APPROACH: SPREADING VELOCITY

In the first part of this section we construct a general formalism to calculate a spreading velocity V and derive scaling relations. Explicit calculations are made on a square lattice in subsequent subsections. The present scheme is quite similar to that for a diffusion coefficient on percolation lattices developed before.[14] The process is described by three basic parameters: a lattice constant l, an infection probability p, and a unit time w which represents a real time necessary to advance one step. All physical quantities including V are determined from l, p, and w. Hereafter we assume the existence of a RSRG transformation. The self-similarity of percolation clusters[15] justifies this assumption. We adopt a usual scheme with a rescaling factor b,

$$l'=bl , \tag{3.1}$$

where a prime denotes a renormalized quantity. The product theorem[16] informs us that recursion relations for p and w have the form

$$p'=g(p,b) , \tag{3.2}$$

$$w'=wf(p,b) . \tag{3.3}$$

It also leads to

$$V(l,p,w;t)=lw^{-1}V^*(p,T) , \tag{3.4}$$

where $T\equiv t/w$, and V^* is a normalized dimensionless velocity. In the spirit of a RSRG approach, relevant macroscopic properties of the process are kept invariant under the transformation, and

$$V(l',p',w';t)=V(l,p,w;t) . \tag{3.5}$$

Substitution of Eqs. (3.1)–(3.4) into Eq. (3.5) gives a recursion relation for V^*

$$V^*(p,T)=bf^{-1}V(g,Tf^{-1}) . \tag{3.6}$$

Here we define V by a time derivative of an average cluster size, e.g., a radius of gyration. Hence, we set

$$V(l,p,w;w)=plw^{-1} , \tag{3.7}$$

because at $t=w$, i.e., after one step, a cluster spreads pl on the average. Iterating the transformation k times and inserting Eq. (3.7), we have

$$V^*(p,T)=p_k\prod_{i=0}^{k-1} b(f(p_i,b))^{-1} , \tag{3.8}$$

$$p_{i+1}=g(p_i) \quad (p_0=p) , \tag{3.9}$$

$$T=T_k=\prod_{i=0}^{k-1} f(p_i,b) . \tag{3.10}$$

Using Eqs. (3.8)–(3.10), we can compute V^* explicitly.

Critical behavior and scaling relations are also derived. In the vicinity of a threshold p_c as $\epsilon\equiv|p-p_c|/p_c\ll 1$, recursion relations (3.2) and (3.3) are expanded as

$$\epsilon'=\lambda_p\epsilon+O(\epsilon^2) , \tag{3.11}$$

$$f=\lambda_w+O(\epsilon) , \tag{3.12}$$

where $\lambda_p\equiv \partial g/\partial p\,|_{p=p_c}$ and $\lambda_w\equiv f\,|_{p=p_c}$. Substituting Eqs. (3.11) and (3.12) into Eq. (3.6), we get

$$V^*(\epsilon,T)=b\lambda_w^{-1}V^*(\lambda_p\epsilon,\lambda_w^{-1}T) . \tag{3.13}$$

Then we find that V^* is a generalized homogeneous function and satisfies scaling relations[17]

$$V^*(\epsilon,T)=\epsilon^{\theta}F(\epsilon T^{\chi/\nu}) \tag{3.14}$$

with critical exponents

$$\theta\equiv \ln(\lambda_w/b)/\ln\lambda_p=\nu(1-\chi)/\chi , \tag{3.15}$$

$$\chi\equiv \ln b/\ln\lambda_w=\nu/(\theta+\nu) , \tag{3.16}$$

where $\nu\equiv\ln b/\ln\lambda_p$ is a correlation-length exponent[13] and

F is a scaling function. Just at a threshold $p=p_c$ and in the long-time limit $T\to\infty$, V^* follows power-law behavior,

$$V^*(p_c,T)\propto T^{\chi-1}\,, \tag{3.17}$$

$$V^*(\epsilon,\infty)\propto\epsilon^{\theta}\,. \tag{3.18}$$

The relaxation time τ of the process is estimated from

$$\xi\propto\epsilon^{-\nu}\sim V\tau\propto\tau^{\chi}\,, \tag{3.19}$$

where ξ is a correlation length and $V\tau$ stands for an average cluster size. Then the critical exponent ψ for τ is expressed as

$$\psi=\theta+\nu=\nu/\chi\,. \tag{3.20}$$

In the perfect immunization process (isotropic percolation), ψ is equal to the minimum path exponent $\zeta_{\min}$,[18] whereas in the no-immunization process (directed percolation), ψ is same as the exponent $\nu_{\|}$ for a correlation length parallel to the anisotropy axis.[6]

A. Perfect immunization process

We now specialize to a square lattice and construct recursion relations as follows. A $b=2$ cell-to-cell decimation procedure is adopted and a group of sites and bonds are combined into supersites and superbonds, as illustrated in Fig. 2.[19] On the original cell, we start with a configuration where only the origin (bottom site) is infected and others are susceptible. The process is advanced until the top site is infected or infected sites become extinct. Then we calculate an infection probability of the top site and equate it to that on the renormalized cell, viz., p'. The resulting recursion relation g for p is

$$p'=g(p)=2p^2+2p^3-5p^4+2p^5\,. \tag{3.21}$$

This recursion relation is same as that for bond percolation[19] and gives the exact threshold

$$p_c=0.5\,. \tag{3.22}$$

Similarly, the recursion relation f for w is obtained by computing an average step number n until the top site is infected and by setting

$$w'n'=wn\,, \tag{3.23}$$

where $n'=1$ is an average number on the renormalized cell. Equation (3.23) means that a real time until infection of the top site is preserved under the transformation. It follows that

$$w'/w=f(p)=2p^2(2+3p-7p^2+3p^3)/g(p)\,. \tag{3.24}$$

Again, the recursion relation $f(p)g(p)$ is equal to that for the minimum path of bond percolation derived by Hong and Stanley.[20]

Recursion relations (3.21) and (3.24) are used to calculate critical exponents, a spreading velocity, and its scaling function. Critical exponents become

$$\nu=1.43\,, \tag{3.25}$$

$$\theta=0.12\,, \tag{3.26}$$

$$\chi=0.92\,, \tag{3.27}$$

$$\psi=1.55\,. \tag{3.28}$$

The value of ψ and, equivalently, θ and χ, has already been obtained by Hong and Stanley,[20] but the following results about V^* are new. The explicit values of $V^*(p,\infty)$ are plotted in Fig. 3. Because of small value of θ, $V^*(p,\infty)$ shows sharp increase near p_c. Figure 4 presents

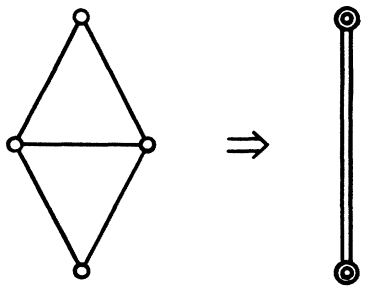

FIG. 2. $B=2$ cell-to-cell decimation scheme.

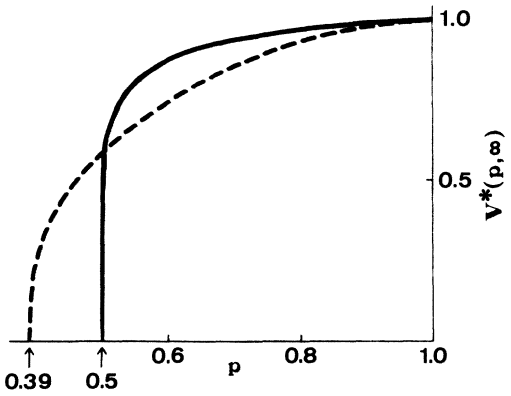

FIG. 3. Asymptotic values of the spreading velocity $V^*(p,\infty)$ for the perfect (——) and the no- (— — —) immunization processes.

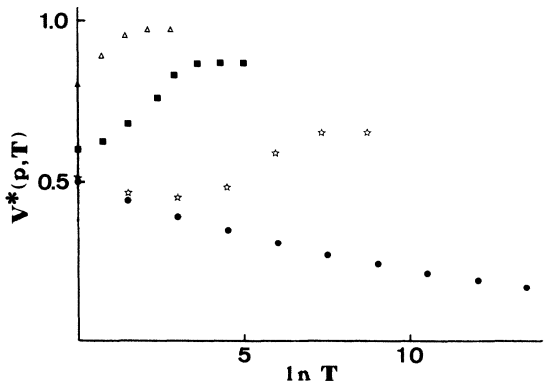

FIG. 4. Time dependence of the spreading velocity $V^*(p,T)$ in the perfect immunization process at $p=0.5$ (●), 0.51 (☆), 0.6 (■), and 0.8 (△).

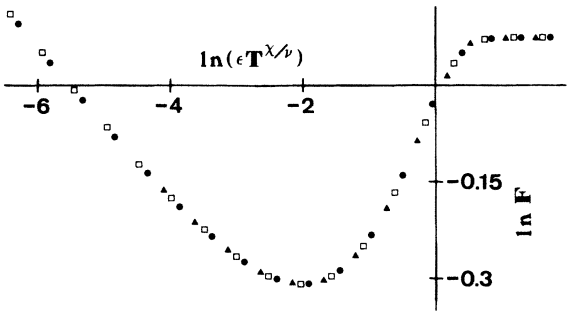

FIG. 5. Scaling function F for the perfect immunization process when $\epsilon=0.01$ (▲), 0.001 (□), and 0.0001 (●).

the time dependence of $V^*(p,T)$. As $p\to p_c$ from above, the relaxation time increases and diverges at $p=p_c$. The scaling function F is shown in Fig. 5. The scaling relation holds well and the crossover occurs smoothly.

B. No-immunization process

The basic scheme for construction of recursion relations in the no-immunization process is same as that in the perfect immunization process. In this case, however, the same configurations appear repeatedly and a self-consistent treatment becomes necessary. Consider a process with m kinds of configurations. Generally, an infection probability P_i^* of the top site after starting with a configuration i is written as

$$P_i^*=P_{i0}+\sum_{j=1}^{m}P_{ij}P_j^* , \tag{3.29}$$

where P_{i0} is a direct infection probability from a configuration i without passing through these m configurations, and P_{ij} is a transition probability from a configuration i to j. Calculations of P_{i0} and P_{ij} are straightforward. By solving the equation system (3.29), therefore, we can obtain an infection probability from arbitrary configuration. A similar formula holds for an average step number N_i^* from a configuration i until infection of the top site,

$$P_i^*N_i^*=P_{i0}N_{i0}+\sum_{j=1}^{m}P_{ij}P_j^*(N_j^*+N_{ij}) , \tag{3.30}$$

where N_{i0} is an average step number from a configuration i without repeating any configuration and N_{ij} is an average step number during the transition from a configuration i to j. Here the term N_{ij} represents the increase of a step number due to the repeat of configurations. Thus, an average step number from any configuration can also be determined from N_{i0} and N_{ij}.

In the no-immunization process, two configurations are repeated and we get

$$p'=g(p)=g_1(p)/g_3(p) , \tag{3.31}$$

$$w'/w=f(p)=[f_1(p)g_1(p)+f_2(p)g_2(p)+f_3(p)g_3(p)]/g_1(p)g_3(p) , \tag{3.32}$$

$$g_1(p)=p^2(2-p^2+p^3-6p^4+13p^5-13p^6+6p^7-p^8) , \tag{3.33}$$

$$g_2(p)=p(1+p^2-p^3-2p^5+7p^6-9p^7+5p^8-p^9) , \tag{3.34}$$

$$g_3(p)=1-p+p^3+6p^4-15p^5+22p^6-34p^7+47p^8-45p^9+26p^{10}-8p^{11}+p^{12} , \tag{3.35}$$

$$f_1(p)=2p^2(2-p+3p^2-7p^3+7p^4-4p^5+5p^6-12p^7+13p^8-6p^9+p^{10}) , \tag{3.36}$$

$$f_2(p)=2p^2(1-p)^2(2-p+4p^5-8p^6+5p^7-p^8) , \tag{3.37}$$

$$f_3(p)=2p^2(1-p)^3(2-p+8p^2-8p^3+10p^4-12p^5+14p^6-13p^7+6p^8-p^9) . \tag{3.38}$$

A threshold and critical exponents are given by

$$p_c=0.39 , \tag{3.39}$$

$$\nu=1.07 , \tag{3.40}$$

$$\theta=0.37 , \tag{3.41}$$

$$\chi=0.74 , \tag{3.42}$$

$$\psi=1.44 . \tag{3.43}$$

The value of $\psi=1.44$ is a little larger than the 1.27 of known estimates.[6] In Fig. 3, $V^*(p,\infty)$ is plotted together with that of the perfect immunization process. The larger value of θ causes the slower increase of $V^*(p,\infty)$ near p_c. The asymptotic value $V^*(p,\infty)$ in the no-immunization process is exactly equal to $\tan\phi$ in directed percolation, where ϕ is the opening angle of the infinite cluster.[6] Hence, Fig. 3 can be regarded as a p-versus-$\tan\phi$ phase diagram of directed percolation, which describes an interesting characteristic of directed percolation, namely direction-dependent critical behavior.[6] The time dependence of $V^*(p,T)$ and the scaling function F are shown in Figs. 6 and 7. The divergence of the relaxation time and the smooth crossover are observed.

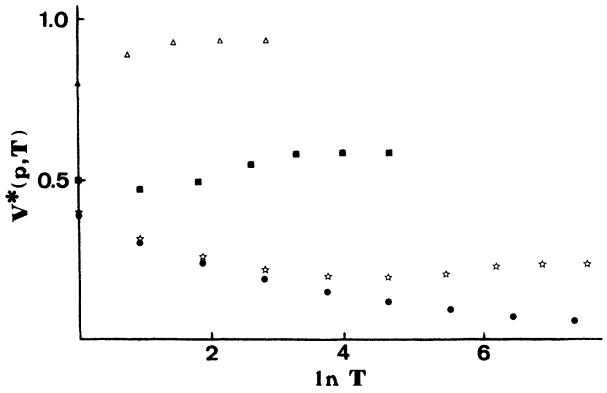

FIG. 6. Time dependence of the spreading velocity $V^*(p,T)$ in the no-immunization process at $p=0.39$ (●), 0.4 (☆), 0.5 (■), and 0.8 (△).

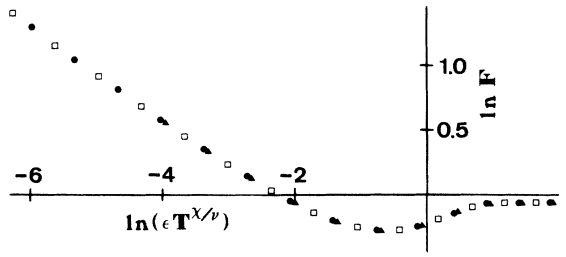

FIG. 7. Scaling function F for the no-immunization process when $\epsilon=0.01$ (▲), and 0.001 (□), and 0.0001 (●).

IV. REAL-SPACE RENORMALIZATION-GROUP APPROACH: PHASE DIAGRAMS AND TRICRITICAL BEHAVIOR

In the partial and imperfect immunization processes, there exists one more parameter u or r in addition to p. This causes tricritical behavior near a tricritical point. As in Sec. III, we first present a general formalism[21] and then make explicit calculations on a square lattice. Consider a two-parameter RSRG transformation with recursion relations

$$x'=g_x(x,y)\ , \tag{4.1}$$

$$y'=g_y(x,y)\ , \tag{4.2}$$

where we denote parameters by x and y. Assuming the existence of an unstable fixed (tricritical) point (x_c,y_c) and linearizing Eqs. (4.1) and (4.2) around (x_c,y_c), we have

$$\begin{bmatrix}\epsilon_x'\\ \epsilon_y'\end{bmatrix}=\Lambda\begin{bmatrix}\epsilon_x\\ \epsilon_y\end{bmatrix}\ , \tag{4.3}$$

$$\Lambda=\begin{bmatrix}\lambda_{xx} & \lambda_{xy}\\ \lambda_{yx} & \lambda_{yy}\end{bmatrix}=\begin{bmatrix}\partial g_x/\partial x & \partial g_x/\partial y\\ \partial g_y/\partial x & \partial g_y/\partial y\end{bmatrix}\Bigg|_{x=x_c,\,y=y_c}\ , \tag{4.4}$$

where $\epsilon_x\equiv(x-x_c)/x_c$ and $\epsilon_y\equiv(y-y_c)/y_c$. Diagonalization of Eq. (4.3) leads to

$$\epsilon_1'=\lambda_1\epsilon_1\ \ (\epsilon_1=A_1\epsilon_x+B_1\epsilon_y)\ , \tag{4.5}$$

$$\epsilon_2'=\lambda_2\epsilon_2\ \ (\epsilon_2=A_2\epsilon_x+B_2\epsilon_y)\ , \tag{4.6}$$

where λ_1 and λ_2 are eigenvalues of Λ and (A_1,B_1) and (A_2,B_2) are eigenfunctions of Λ. Critical behaviors of physical quantities are derived from Eqs. (4.5) and (4.6). Here we discuss a correlation length ξ and a spreading velocity V. The product theorem[16] and the invariance under the transformation yields

$$\xi(l',x',y')=\xi(l,x,y)=l\xi^*(x,y)\ , \tag{4.7}$$

where ξ^* is a normalized dimensionless length. Inserting Eqs. (3.1), (4.5), and (4.6) into Eq. (4.7), we get

$$\xi^*(\epsilon_1,\epsilon_2)=b\xi^*(\lambda_1\epsilon_1,\lambda_2\epsilon_2)\ . \tag{4.8}$$

Then ξ^* has the scaling form[17]

$$\xi^*(\epsilon_1,\epsilon_2)=\epsilon_1^{-\nu_1}F_\xi(\epsilon_1^{\nu_1}\epsilon_2^{-\nu_2}) \tag{4.9}$$

with critical exponents

$$\nu_1=\ln b/\ln\lambda_1\ , \tag{4.10}$$

$$\nu_2=\ln b/\ln\lambda_2\ . \tag{4.11}$$

Along the line $\epsilon_2=0$ or $\epsilon_1=0$, ξ^* obeys

$$\xi^*(\epsilon_1,0)\propto\epsilon_1^{-\nu_1}\ , \tag{4.12}$$

$$\xi^*(0,\epsilon_2)\propto\epsilon_2^{-\nu_2}\ . \tag{4.13}$$

Similarly, Eqs. (3.4) and (3.5) are generalized as

$$V(l',x',y',w';t)=V(l,x,y,w;t)=lw^{-1}V^*(x,y,T)\ . \tag{4.14}$$

It follows that

$$V^*(\epsilon_1,\epsilon_2,T)=b\lambda_w^{-1}V^*(\lambda_1\epsilon_1,\lambda_2\epsilon_2,\lambda_w^{-1}T) \tag{4.15}$$

and

$$V^*(\epsilon_1,\epsilon_2,T)=T^{\chi-1}F_V(\epsilon_1T^{\chi/\nu_1},\epsilon_2T^{\chi/\nu_2})\ , \tag{4.16}$$

$$V^*(0,0,T)\propto T^{\chi-1}\ , \tag{4.17}$$

$$V^*(\epsilon_1,0,\infty)\propto\epsilon_1^{\theta_1}\ , \tag{4.18}$$

$$V^*(0,\epsilon_2,\infty)\propto\epsilon_2^{\theta_2} \tag{4.19}$$

with

$$\theta_1=\ln(\lambda_w/b)/\ln\lambda_1=\nu_1(1-\chi)/\chi\ , \tag{4.20}$$

$$\theta_2=\ln(\lambda_w/b)/\ln\lambda_2=\nu_2(1-\chi)/\chi\ . \tag{4.21}$$

A. Partial immunization process

To construct a recursion relation g_p for p, we apply the same scheme as in Sec. III. Extension is lengthy but straightforward. As for g_u, we compute an immunization probability of the origin until the infection of the top site or the extinction of infected sites on the original cell and set it equal to that u' on the renormalized cell. Here four configurations appear repeatedly and obtained recursion relations are rather complicated. Full expressions are presented in the Appendix. Using these recursion relations, we can calculate a global phase diagram. The result is shown in Fig. 8. Qualitative properties are same as those by the mean-field theory [Fig. 1(a)] and two phases appear. In phase I, $p\to0$ and the disease spreads only finitely, while in phase II, $p\to1$ and infinite spreading can occur. It should be noted that except at $u=0$, u always goes to unity and the partial immunization process belongs to the same universality class as that of the perfect immunization process. The tricritical point is

$$p_c=0.39,\ \ u_c=0\ . \tag{4.22}$$

Eigenvalues and eigenfunctions of the linearized transformation matrix and critical exponents are given by

$$\lambda_1=1.91\ , \tag{4.23}$$

$$(A_1,B_1)=(1,0)\ , \tag{4.24}$$

$$\nu_1=1.07\ , \tag{4.25}$$

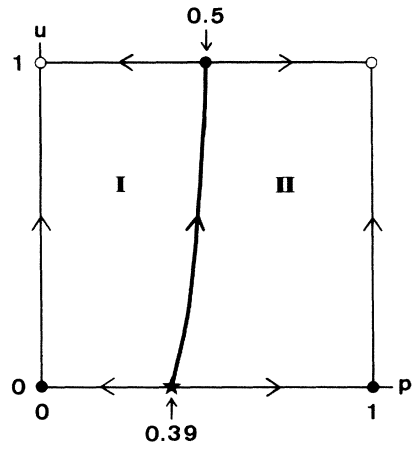

FIG. 8. Phase diagram of the partial immunization process using the RSRG method. The star (★), solid circles (●), and open circles (○) denote the tricritical, other unstable, and stable fixed points, respectively.

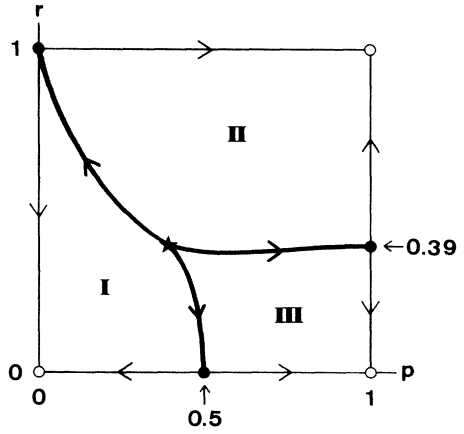

FIG. 9. Same as Fig. 8 for the imperfect immunization process.

$$\theta_1=0.37\ , \tag{4.26}$$

and

$$\lambda_2=1.37\ , \tag{4.27}$$

$$(A_2,B_2)=(1,3.28)\ , \tag{4.28}$$

$$\nu_2=2.22\ , \tag{4.29}$$

$$\theta_2=0.78\ . \tag{4.30}$$

Both eigenvalues are more than unity. Then we find that the fixed point (4.22) is truly tricritical and both parameters p and u are relevant.[21] The former behavior is observed along the line $u=0$ and equal to that of the no-immunization process.

B. Imperfect immunization process

Again, a recursion relation g_p for p is determined in the same way as before, whereas g_r for r is obtained as follows. On the original cell, we start with a configuration where the origin (bottom site) is infected, the top site is immune, and the middle two sites are susceptible or immune. An infection probability of the top site is calculated for each configuration of the middle sites and an average is taken over all configurations. As a weight for the average, we use the probability that each configuration is realized as a final configuration of the process in calculations of g_p. Finally, we equalize the average probability to that r' on the renormalized cell. Explicit formulas of g_p and g_r are given in the Appendix.

Figure 9 shows a global phase diagram. As in the mean-field diagram [Fig. 2(b)], there exist three phases. Phase I is a nonpercolating phase where $p\to 0$, $r\to 0$, and only a finite cluster is formed. Phases II and III are percolating phases where $p\to 1$ and an infinite cluster can be formed. In phase II, r also goes to unity and infected sites can survive forever. In phase III, conversely, r goes to zero and reinfection of immune sites is prohibited. Then we find that in the length scale larger than a correlation length ξ, infected sites remain only at the perimeter of the cluster, as suggested before. Recent field-theoretical approaches have shown that the epidemic process with immunization belongs to the same universality class as that of isotropic percolation.[3] However, this statement is true only for the perfect immunization process. When reinfection is allowed, the situation is not so simple. It should be emphasized that the present diagram satisfies two qualitative conditions. One is that on the line $r=1$ the critical point must be $p=0$, because in this case the disease spread once never disappears. The other is that at $p=1$ the critical value of r (threshold) must coincide with that of the no-immunization process. Here the disease spreads infinitely with the velocity $V^*=1$. The formed cluster is compact and composed only of infected and immune sites. In addition, susceptible sites outside the cluster have no influence on the reinfection process of immune sites inside the cluster, because the spreading velocity of the reinfection is always less than unity, i.e., the spreading velocity of the cluster itself. As a result, reinfection process inside the cluster is equivalent to the no-immunization process. The latter condition is satisfied by the mean-field diagram but the former is not.

The tricritical point is

$$p_c=r_c=0.39\ , \tag{4.31}$$

and tricritical behavior is described by

$$\lambda_1=1.91\ , \tag{4.32}$$

$$(A_1,B_1)=(1,1)\ , \tag{4.33}$$

$$\nu_1=1.07\ , \tag{4.34}$$

$$\theta_1=0.37\ , \tag{4.35}$$

$$\lambda_2=1.48\ , \tag{4.36}$$

$$(A_2,B_2)=(1,-0.52)\ , \tag{4.37}$$

$$\nu_2=1.77\ , \tag{4.38}$$

$$\theta_2=0.62\ . \tag{4.39}$$

As in the partial immunization process, both eigenvalues are more than unity and Eq. (4.31) describes the true tricritical point. The first behavior appears along the line $r=p$ and is the same as that of the no-immunization process. On the other hand, the second is observed when the tricritical point is approached via phase III.

V. SUMMARY AND DISCUSSIONS

KGP is a kinetic growth process which shows a percolating-nonpercolating phase transition. The main concern is conditions for the infinite growth and critical behavior near thresholds. Such growth phenomena are observed in a number of fields including physics, chemistry, biology, and even social sciences. In this paper, we have investigated several examples describing epidemic processes with immunization and calculated phase diagrams, critical exponents, and spreading velocities. As a result, the existence and the nature of phase transitions and critical behavior have been clarified.

The partial immunization process where perfect immunization occurs with probability u has only two phases, the nonpercolating phase I and the percolating phase II, and belongs to the same universality class as that of the perfect immunization process (isotropic percolation). On the other hand, three phases appear in the imperfect immunization process, where immune sites are reinfected with probability r. Phase I is a nonpercolating phase where the disease spreads just finitely, and phases II and III are percolating phases with a nonzero probability of infinite spreading of the disease. However, there is significant difference between phases II and III. In phase II infected sites can survive forever in the whole cluster, whereas in phase III infected sites can exist only at the perimeter of the cluster. It becomes evident that reinfection of immune sites is an important factor which causes a qualitative change of the process.

First, we have adopted the mean-field approximation. A mean-field theory is the most fundamental and well-established approach to phase transitions, and most of the existing studies about nonequilibrium phase transitions are based upon it. As is shown in thermal critical phenomena, however, spatial fluctuations are considered to play a crucial role and cause nonclassical behavior near critical points.[11] Then we developed the RSRG technique and obtained nonclassical exponents, etc. The importance of spatial fluctuations has been revealed and a RSRG method has turned out to be a powerful tool in the study of nonequilibrium and irreversible processes as well as of thermal and geometrical (percolative) critical phenomena.

There is some analogy between tricritical behavior of the imperfect immunization process and that of usual thermal systems such as ^{3}He-^{4}He mixtures and metamagnets. In general, thermal tricritical points are located at the end of coexistence curves of three phases characterized as disordered, ordered, and inhomogeneous (separated) phases.[22] In phase III of the imperfect immunization process, infected sites exist only at the perimeter and the cluster is inhomogeneous. In other words, phase separation between infected and immune sites occurs. Then phases I, II, and III correspond to disordered, ordered, and inhomogeneous phases, respectively.

Throughout this article we have used the language of epidemic processes. As mentioned first, however, all expressions can be translated into the language of (autocatalytic) chemical reactions. The partial immunization process is described by

$$X+Y\overset{p}{\rightarrow}2Y\ , \tag{5.1}$$

$$Y\overset{1-u}{\rightarrow}X\ , \tag{5.2}$$

$$Y\overset{u}{\rightarrow}Z\ , \tag{5.3}$$

and the imperfect immunization process is written as

$$X+Y\overset{p}{\rightarrow}2Y\ , \tag{5.4}$$

$$Y\overset{1}{\rightarrow}Z\ , \tag{5.5}$$

$$Z+Y\overset{r}{\rightarrow}2Y\ . \tag{5.6}$$

The mean-field equations (2.1)—(2.3) and (2.18)—(2.20) express usual rate equations for these reactions. Here the issue is whether the reactions proceed infinitely or not when one Y (autocatalytic) molecule is put in the sea of X (reactant) molecules. The similar situation is thought to be realized in a wide variety of real chemical reactions.

The study of growth processes from a viewpoint of KGP seems to be quite interesting both theoretically and practically, but this promising field of research has just begun. Various types of applications are possible and many open questions remain. We hope that this work stimulates further researches on KGP.

ACKNOWLEDGMENT

This work was supported in part by the National Science Foundation under Grant No. CHE84-11303.

APPENDIX: RECURSION RELATIONS

1. Partial immunization process

We have

$$p'=g_p(p,u)=\frac{[(1-P_{22})P_1+P_{12}P_2]}{[(1-P_{11})(1-P_{22})-P_{12}P_{21}]}\ ,$$

$$P_1=P_{10}+P_{13}P_3+P_{14}P_4\ ,$$

$$P_2=P_{20}+P_{23}P_3+P_{24}P_4\ ,$$

$$P_3=P_{30}/(1-P_{33})\ ,$$

$$P_4=P_{40}/(1-P_{44})\ ,$$

$$1-P_{11}=1-v^3p^2q^2(1-q^2)\ ,$$

$$1-P_{22}=1-vpq^2-v^3p^2q^2(1-q^2)\ ,$$

$$1-P_{33}=1-vpq\ ,$$

$$1-P_{44}=1-uvpq^2\ ,$$

$$P_{12}=2vpq\ ,$$

$$P_{21}=vpq^2\ ,$$

$$P_{13}=2upq ,$$
$$P_{14}=2u^2v^2p^2q^3(1-q^2) ,$$
$$P_{23}=uv^2p^2q^2(1-q^2) ,$$
$$P_{24}=upq^2+u^2pq^3+uv^2p^2q^2(1-q^2) ,$$
$$P_{10}=p^2(1-q^2)+2u^2v^2p^4q^2(1-q^2) ,$$
$$P_{20}=p+p^3q+u^2p^3q^2+u^2vp^3q^2(1-q^2) ,$$
$$P_{30}=p+up^2q ,$$
$$P_{40}=p+uvp^3q ,$$
$$u'=g_u(p,u)=\frac{[(1-P_{22})U_1+P_{12}U_2]}{[(1-P_{11})(1-P_{22})-P_{12}P_{21}]} ,$$
$$U_1=U_{10}+P_{13}U_3+P_{14}U_4 ,$$
$$U_2=U_{20}+P_{23}U_3+P_{24}U_4 ,$$
$$U_3=U_{30}/(1-P_{33}) ,$$
$$U_4=U_{40}/(1-P_{44}) ,$$
$$U_{10}=u(p^2+q^2)+uvp^2(1-q^2)(1-v^2q^2) ,$$
$$U_{20}=up^2+u^2pq+uvp^2q(1-vq+vq^3) ,$$
$$U_{30}=1-vpq ,$$
$$U_{40}=up ,$$
$$q=1-p ,$$
$$v=1-u .$$

2. Imperfect immunization process

We have

$$p'=g_p(p,r)=P_{12}P_2+P_{13}P_3 ,$$
$$P_2=(P_{20}+P_{23}P_3+P_{24}P_4)/(1-P_{22}) ,$$
$$P_3=\frac{[(1-P_{44})P_{30}+P_{34}P_{40}]}{[(1-P_{33})(1-P_{44})-P_{34}P_{43}]} ,$$
$$P_4=\frac{[(1-P_{33})P_{40}+P_{43}P_{30}]}{[(1-P_{33})(1-P_{44})-P_{34}P_{43}]} ,$$
$$1-P_{22}=1-q^3r^2 ,$$
$$1-P_{33}=1-q^2r^2(1-s^2) ,$$
$$1-P_{44}=1-qr(s+2rs^2+qr-qrs^2) ,$$
$$P_{12}=2pq ,$$
$$P_{13}=p^2 ,$$
$$P_{23}=pq^2r^2 ,$$
$$P_{24}=pqs+pq^2r(1+s-s^2) ,$$
$$P_{34}=2q^2rs(1-s^2) ,$$
$$P_{43}=qr^3s ,$$
$$P_{20}=p+p^2qr ,$$
$$P_{30}=1-q^2 ,$$
$$P_{40}=p+pqr^2 ,$$
$$r'=g_r(p,r)=R_0R_1+(1-R_0)R_3 ,$$
$$R_0=2p^2q^2/[(1-q^3r^2)g_p(p,r)] ,$$
$$R_1=(R_{10}+R_{12}R_2+R_{13}R_3)/(1-R_{11}) ,$$
$$R_2=\frac{[(1-R_{33})R_{20}+R_{23}R_{30}]}{[(1-R_{22})(1-R_{33})-R_{23}R_{32}]} ,$$
$$R_3=\frac{[(1-R_{22})R_{30}+R_{32}R_{20}]}{[(1-R_{22})(1-R_{33})-R_{23}R_{32}]} ,$$
$$1-R_{11}=1-q^2r^2s ,$$
$$1-R_{22}=1-rs^2(1+r-rs^2) ,$$
$$1-R_{33}=1-r^2s^2(1-s^2) ,$$
$$R_{12}=ps+pqrs^2(1+r-rs^2) ,$$
$$R_{13}=prs^2(1-s^2) ,$$
$$R_{23}=rs^2 ,$$
$$R_{32}=2rs ,$$
$$R_{10}=qr^2+pqr^3s+pr(1-s^2) ,$$
$$R_{20}=r+r^3s ,$$
$$R_{30}=r^2(1-s^2) ,$$
$$q=1-p ,$$
$$s=1-r .$$

[1]Z. Alexandrowicz, Phys. Lett. **80A**, 284 (1980).

[2]P. Grassberger, Math. Biosci. **63**, 157 (1983); G. Mackay and N. Jan, J. Phys. A **17**, L757 (1984).

[3]H. K. Janssen, Z. Phys. B **58**, 311 (1985); J. L. Cardy and P. Grassberger, J. Phys. A **18**, L267 (1985).

[4]P. Grassberger and K. Sundermeyer, Phys. Lett. **77B**, 220 (1978); H. K. Janssen, Z. Phys. B **42**, 151 (1981); J. L. Cardy and R. L. Sugar, J. Phys. A **13**, L423 (1980).

[5]P. Grassberger and A. de la Torre, Ann. Phys. (N.Y.) **122**, 373 (1979).

[6]W. Kinzel, Ann. Israel Phys. Soc. **5**, 425 (1983).

[7]J. L. Cardy, J. Phys. A **16**, L709 (1983).

[8]F. Schlögl, Z. Phys. **253**, 147 (1972).

[9]See, e.g., D. Wilkinson and J. F. Willemsen, J. Phys. A **16**, 3365 (1983); A. R. Kerstein, Phys. Rev. B **30**, 2980 (1984); L. S. Schulman and P. E. Seiden, Ann. Israel Phys. Soc. **5**, 251 (1983).

[10]*Kinetics of Aggregation and Gelation,* edited by F. Family and

D. P. Landau (North-Holland, Amsterdam, 1984).
[11]G. Nicolis and I. Prigogine, *Self-Organization in Nonequilibrium Systems* (Wiley, New York, 1977); H. Haken, *Synergetics* (Springer, Berlin, 1978).
[12]S. Wolfram, Rev. Mod. Phys. **55**, 601 (1983); W. Kinzel, Z. Phys. B **58**, 229 (1985).
[13]D. Stauffer, Phys. Rep. **54**, 1 (1979).
[14]T. Ohtsuki and T. Keyes, Phys. Lett. **104A**, 77 (1984).
[15]A. Kapitulnik, A. Aharony, G. Deutscher, and D. Stauffer, J. Phys. A **16**, L269 (1983).
[16]G. I. Barenblatt, *Similarity, Self-Similarity and Intermediate Asymptotics* (Consultants Bureau, New York, 1979).
[17]H. E. Stanley, *Introduction to Phase Transitions and Critical Phenomena* (Clarendon, Oxford, 1971).
[18]R. Pike and H. E. Stanley, J. Phys. A **14**, L169 (1981).
[19]P. J. Reynolds, W. Klein, and H. E. Stanley, J. Phys. C **10**, L167 (1977); H. E. Stanley, P. J. Reynolds, S. Redner, and F. Family, in *Real-Space Renormalization,* edited by T. W. Burkhardt and J. M. J. van Leeuwen (Springer, Berlin, 1982).
[20]D. C. Hong and H. E. Stanley, J. Phys. A **16**, L525 (1983).
[21]See, e.g., D. J. Wallace and R. K. P. Zia, Rep. Prog. Phys. **14**, 1 (1978).
[22]I. D. Lawrie and S. Sarbach, in *Phase Transitions and Critical Phenomena,* edited by C. Domb and J. L. Lebowitz (Academic, London, 1984), Vol. 9.